Macromolecules 1989, 22, 2438–2446

Stereocomplexation of Isotactic Polyesters of Opposite Configurations

Claude Lavallée and Robert E. Prud'homme*

Département de Chimie, Centre de Recherche en Sciences et Ingénierie des Macromolécules, Université Laval, Sainte-Foy, Québec, Canada G1K 7P4. *Received July 19, 1988; Revised Manuscript Received October 21, 1988*

ABSTRACT: Blends of isotactic poly(α-methyl-α-ethyl-β-propiolactones) (PMEPL) of opposite configurations and high optical purities lead to the formation of a stereocomplex. This complex melts 40 °C above the melting temperature of the corresponding isotactic polymers and is characterized by a unique X-ray diffraction pattern and a spherulitic morphology. In this article, blends of PMEPL have been prepared, keeping the tacticity of one component constant and changing the other one from the isotactic polymer to the completely atactic one. These mixtures have been characterized by differential scanning calorimetry, X-ray diffraction, and polarized microscopy. In most cases, the melting temperature of the blends is above those of the corresponding pure components, with characteristic X-ray diffraction patterns and morphologies, indicating also the formation of a stereocomplex. However, the melting point of the complex and the size of the spherulites decrease with a decrease of isotacticity. The stereocomplex is always preferentially formed (over the crystallization of the isotactic polymers), even in nonequimolar blends, and it controls the morphology over a wide range of concentration. Melting point depression data have been analyzed by using the Sanchez–Eby copolymer crystallization theory. The free enthalpy of incorporation of the heterotactic units has been evaluated at about 5.7 kJ/mol. It corresponds to the incorporation of at least 50% of the heterotactic units into the stereocomplex.

Introduction

Several molecules spontaneously form complexes in bulk or in solution. For example, metallic alloys and racemic organic compounds form complexes which have different properties than those of the corresponding pure compounds.[1] However, there are few examples of macromolecular complexes. Poly(ethylene oxide) and poly(acrylic acid) form an amorphous complex upon mixing in solution.[2] Also, when a solution of isotactic poly(methyl methacrylate) (PMMA) and a solution of syndiotactic PMMA are mixed, a white semicrystalline precipitate appears.[3] Such a complex between two tactic samples of a polymer is often called a stereocomplex.

There are few cases of stereocomplexation between two isotactic polymers of opposite configurations, also called a polyracemate complex: poly(*tert*-butylthiirane),[4] poly(α-methylbenzyl methacrylate),[5] poly(lactide),[6] and poly(α-methyl-α-ethyl-β-propiolactone) (PMEPL).[7] In contrast, mixtures of polyenantiomers of poly(propylene oxide) and poly(methylthiirane) do not show any evidence of complex formation.[8]

Recently, Grenier et al. have reported the synthesis of PMEPL's[9] of different degrees of tacticity, going from the atactic polymer to the completely isotactic one. They have also reported, as mentioned above, the formation of a polyracemate complex.[7] The properties of this complex differ from those of the corresponding pure polymers. For example, the atactic polymer melts at 121 °C, the isotactic polymer at 164 °C, and the stereocomplex at 202 °C. The polyracemate also shows a different morphology and X-ray diffraction patterns than its pure components. In order to gain a better understanding of the stereocomplexation phenomenon and to better define its limits, blends of PMEPL's with different tacticities were prepared, in this article, and analyzed by differential scanning calorimetry, X-ray diffraction, and polarized microscopy. Melting point depression data were then related to the isotacticity and average isotactic sequence length of the chains.

Experimental Section

The polymers used in this study have been prepared by Grenier et al.[9] and are described in Table I. The acronyms used refer to the enantiomeric excess (e.e.) of the samples and give the isomer in excess. For example, a polymer containing 77.5% of the *S* isomer and 22.5% of the *R* isomer is called PMEPL-55S where 55 is the enantiomeric excess of the *S* isomer since e.e. = 77.5–22.5 = 55. These polymers have been prepared by a mechanism which follows bernoullian statistics,[9] and therefore, their isotacticity is directly related to the enantiomeric composition of the monomer used, which is given by the enantiomeric excess. For example, a racemic compound leads to an atactic polymer which has an enantiomeric excess of 0%, whereas a pure isomer leads to an isotactic polymer with an enantiomeric excess of 100%. Although the enantiomeric excess is not strictly speaking an isotacticity measurement, for the sake of simplicity, these two parameters will be considered equivalent in this article. Table I also gives the average length of the isotactic sequences (in base units) of the samples used.

Polyracemates have been prepared by mixing polymers of opposite configurations and are described by acronyms which are related to the constitutive polymers. As an example, the mixing of PMEPL-97R and PMEPL-55S leads to a polyracemate called PMEPL-97R/55S. Furthermore, the composition of the polyracemates is always specified by the weight percent of homopolymer of *R* configuration. For example, the mixing of 30 mg of PMEPL-97R with 70 mg of PMEPL-55S gives a polyracemate called PMEPL-97R/55S 30%. This nomenclature is not exactly the same as that used previously by Grenier and Prud'homme.[7]

The polyracemates were prepared as follows: two separate 1% polymer solutions were made in hexafluoro-2-propanol, filtered through micropore (1-μm) filters and mixed together in the proper ratio for 1 h. They were then precipitated in methanol, centrifuged at 7000 rpm for 10 min, and dried at 40 °C under vacuum.

Differential scanning calorimetry (DSC) measurements were conducted with a Perkin-Elmer DSC-4 apparatus calibrated with pure indium. The samples were melted and cooled rapidly to the crystallization temperature (T_c) for 10 min. Melting curves were then recorded at a heating rate of 20 °C/min; the melting temperature was usually read at the end of the melting peak. For comparison purposes, a crystallization temperature of 40 °C below the melting temperature was usually taken; however, for blends containing PMEPL-25S or PMEPL-0S, a crystallization temperature of 80 °C was preferred to avoid the crystallization of PMEPL-97R.

The morphology of the samples was studied with a Zeiss polarizing microscope. For these studies, samples were melted on a Mettler hot stage at 240 °C for 30 s, cooled rapidly to 220 °C, and then cooled slowly to room temperature at a rate of 0.2 °C/min.

X-ray diffraction measurements were conducted with a Rigaku Rotaflex apparatus made of a rotating anode generator, a Cu Kα target, a nickel filter, and a wide-angle goniometer. The samples were melted on a Mettler hot stage between two glass slides at 220 °C and crystallized under the same conditions as those used for the DSC analysis. The $\Delta H_f°$ value used in the melting point depression analysis has been evaluated by extrapolation of the

0024-9297/89/2222-2438$01.50/0

Table I
Characteristics of the Polymers Used

polymer	[R]/%	[S]/%	av isotactic sequence length/base unit	M_n/(kg/mol)	T_f/°C	ΔH_f/(J/g)
PMEPL-97R	98.5	1.5	66.7	49	164	61
PMEPL-53R	76.5	23.5	4.3		124	33
PMEPL-99S	0.5	99.5	200.0	50	164	61
PMEPL-75S	12.5	87.5	8.0	41	137	43
PMEPL-55S	22.5	77.5	4.4	29	124	33
PMEPL-25S	37.5	62.5	2.7	40	122	33
PMEPL-0S	50.0	50.0	2.0	300	118	32

Table II
Melting Temperature of 50% PMEPL-R/PMEPL-S Blends and of Their Corresponding PMEPL Components

	melting temp, °C		
	component		
blend	R	S	stereocomplex
PMEPL-97R/99S	164	164	196
PMEPL-97R/75S	164	137	180
PMEPL-97R/55S	164	124	172
PMEPL-97R/25S	164	122	157
PMEPL-97R/0S	164	118	≈145
PMEPL-53R/99S	124	164	172
PMEPL-53R/75S	124	137	169
PMEPL-53R/55S	124	124	157
PMEPL-53R/25S	124	122	138
PMEPL-53R/0S	124	118	128

inverse of the DSC enthalpy of fusion of samples of pure complexes plotted as a function of the amorphous/crystalline ratio of the X-ray diffraction pattern; a value of 22.4 kJ/mol was then found.

Results and Discussion

DSC Analysis. Figure 1 gives the DSC melting curves of the polymers used and of some of the mixtures. Several blends exhibit a melting temperature above those of the corresponding polymers. For example, PMEPL-97R/99S, PMEPL-97R/75S, and PMEPL-97R/55S (50% blends) melt at 196, 180, and 172 °C, respectively, which are 32, 16, and 8 °C above the melting temperature of the PMEPL-97R polymer. This is taken as evidence of the stereocomplexation of the polymers involved since, in addition, the melting peaks of the corresponding polymers are not observed. The melting temperatures of all mixtures investigated are reported in Table II. Please note that the melting temperature of the PMEPL-97R/99S complex reported herein is not an equilibrium value and is, therefore, 7 °C below the equilibrium melting temperature reported by Grenier and Prud'homme.[7] For PMEPL-97R/25S, a melting temperature of 157 °C is observed which is intermediate between those of the corresponding polymers. This is also taken as evidence of stereocomplexation since, without complexation, the melting peaks of each component would be seen. Finally, PMEPL-97R/0S shows three melting peaks at about 130, 145, and 155 °C, which are assigned to PMEPL-0S, to the polyracemate complex, and to PMEPL-97R, respectively. Therefore, each of these blends forms, at least in part, a stereocomplex, although the results obtained with PMEPL-97R/25S and PMEPL-97R/0S are more ambiguous than those obtained with the higher tacticity polymers.

The melting curves of several 50% blends prepared with PMEPL-53R are given in Figure 2. These blends exhibit only one melting peak, with a melting temperature above those of the corresponding polymers (Table II). This behavior is associated with stereocomplexation. However, the melting temperature decreases with a decrease in isotacticity of the PMEPL-S component. PMEPL-53R/99S melts at 172 °C, which is identical with PMEPL-97R/55S (although the shape and breadth of the melting peak is slightly different), but the melting temperature decreases to 128 °C with PMEPL-53R/0S, which is only 4 °C above that of PMEPL-53R. In general, the behavior of both series of mixtures, PMEPL-97R/xS and PMEPL-53R/xS where x is the enantiomeric excess of the PMEPL-S component of the mixture, is very similar, and therefore, the remainder of this study will be limited to a detailed analysis of the former mixture which gives larger enthalpies of fusion.

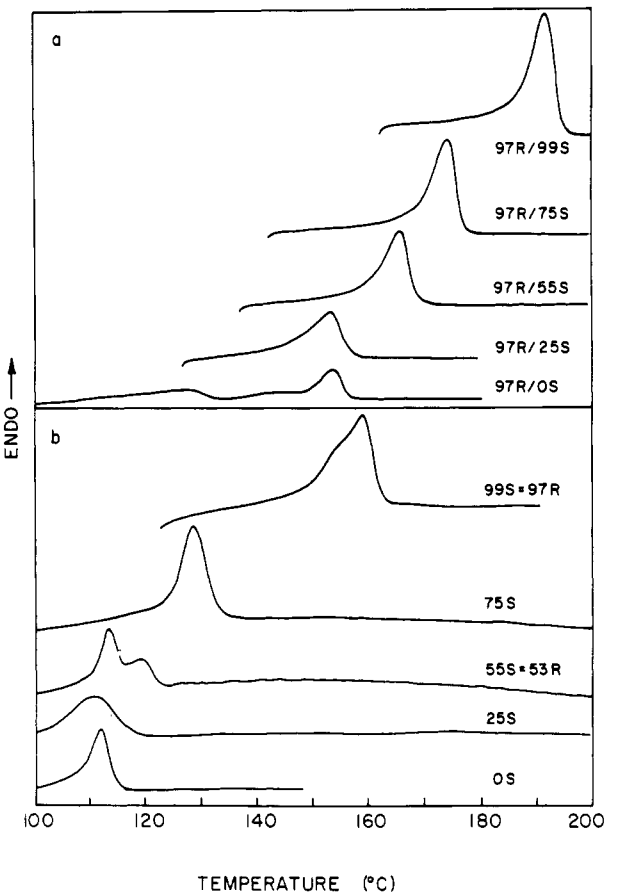

Figure 1. DSC curves of PMEPL samples run at 20 °C/min: (a) blends containing 50% PMEPL-97R; (b) pure PMEPL's.

In order to better understand the stereocomplexation phenomenon, melting curves of PMEPL-97R/75S blends containing 50%, 77%, 91%, 93%, and 100% of PMEPL-97R were obtained (Figure 3). Two peaks are in general present and can be associated to the polymer in excess and to the stereocomplex. The decrease in intensity of the peak at 180 °C (stereocomplex) and the increase in intensity of the peak at 164 °C (PMEPL-97R) with the PMEPL-97R concentration is related to the fraction of each species.

The melting temperatures of these blends are reported as a function of composition in Figure 4 (incidently, this

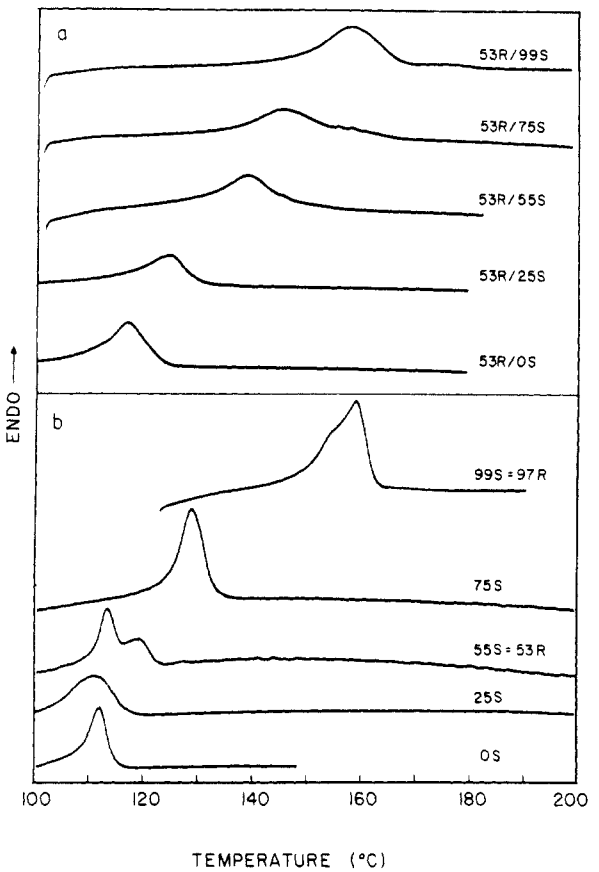

Figure 2. DSC curves of PMEPL samples run at 20 °C/min: (a) blends containing 50% PMEPL-53R; (b) pure PMEPL's.

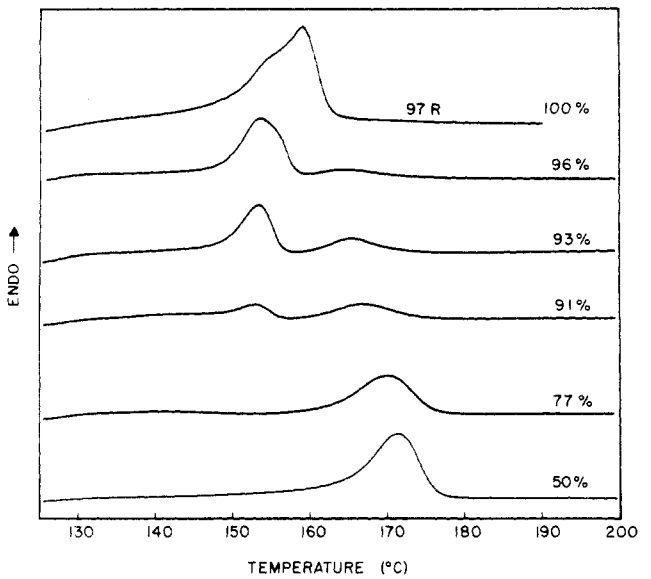

Figure 3. DSC curves of PMEPL-97R/75S samples run at 20 °C/min after crystallization at 120 °C.

figure represents the right-hand side of a standard phase diagram). The melting temperature of the stereocomplex remains constant for most blends but decreases at high concentrations of PMEPL-97R. In contrast, the melting temperature of PMEPL-97R is present only at high concentrations. This behavior is similar to the one reported by Grenier and Prud'homme[7] for PMEPL-97R/99S mixtures. It is very different from that observed with enantiomeric blends of small molecules but seems typical for polymers.

Figure 5 shows that the enthalpy of fusion of the stereocomplex decreases linearly (within the experimental

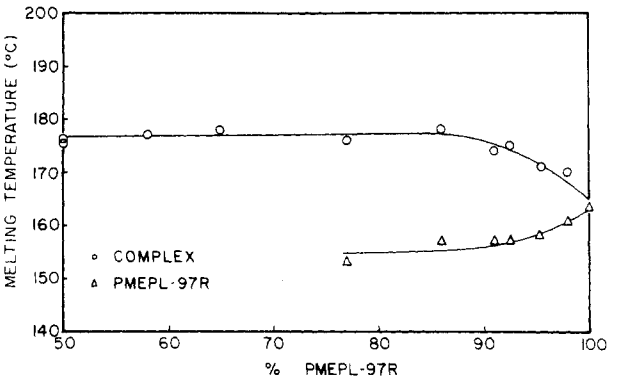

Figure 4. Melting temperature of PMEPL-97R/75S samples crystallized at $T_c = T_f - 40$.

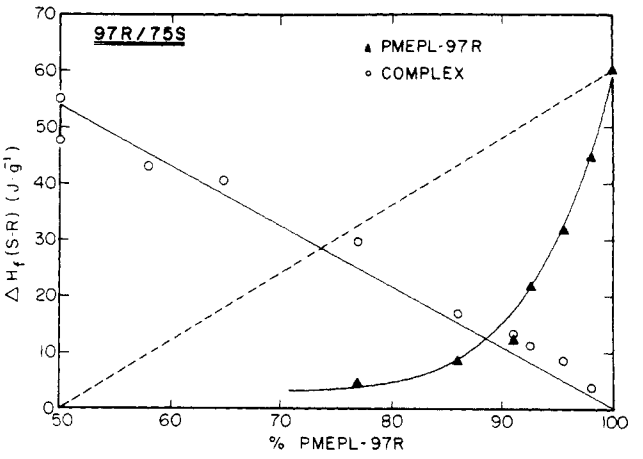

Figure 5. Enthalpy of fusion of PMEPL-97R/75S samples crystallized at $T_c = T_f - 40$.

uncertainty) from 55 to 0 J/g as the concentration of PMEPL-97R is increased from 50% to 100%; this result indicates that the polyracemate is preferentially formed in a constant nearly 1:1 molar ratio. However, the enthalpy of fusion of PMEPL-97R decreases rapidly with composition, with no crystallization at all at concentrations smaller than 75% in PMEPL-97R; the values obtained are always much smaller than those expected considering the amount of PMEPL-97R in excess in the mixtures (this calculation corresponds to the dashed line).

These values of melting temperature (Figure 4) and enthalpy of fusion (Figure 5) can be rationalized by considering that, upon cooling the mixture from the melt, the stereocomplex crystallizes first and leaves a rigid matrix, at least much more rigid than it was before crystallization. The crystallization of the excess polymer, which occurs at a lower temperature, is then hindered to the point where a fraction of the sample which ought to crystallize remains amorphous at high PMEPL-97R concentrations, and where the uncomplexed part of the sample does not crystallize at all at lower concentrations. This explanation will be supported, in the next section, by morphological observations.

PMEPL-97R/55S mixtures were not studied as a function of composition because the melting temperature of the complex is only 8 °C above that of PMEPL-97R, which makes the analysis of the results uncertain.

The melting curves of PMEPL-97R/25S blends are shown in Figure 6 as a function of the PMEPL-97R composition. The melting peak of the stereocomplex, at 157 °C (the peak maximum is at 145 °C), appears below the melting peak of PMEPL-97R, at 164 °C (and above that of PMEPL-25S at 122 °C), and is indicated by arrows for PMEPL-97R compositions between 10% and 90%. Since

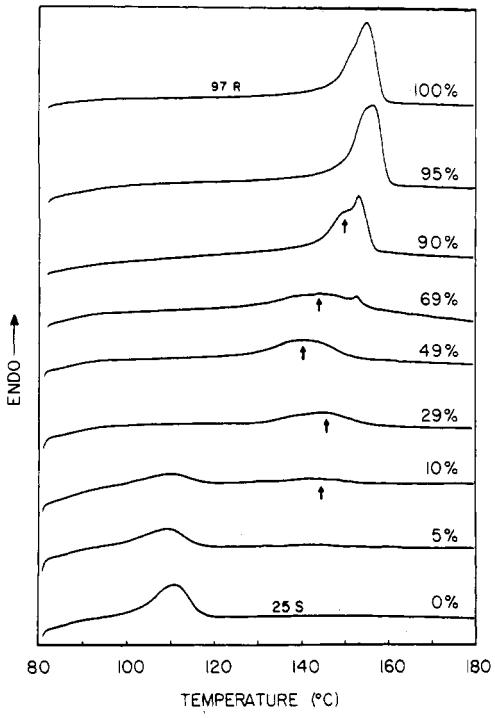

Figure 6. DSC curves of PMEPL-97R/25S samples run at 20 °C/min after crystallization at 80 °C.

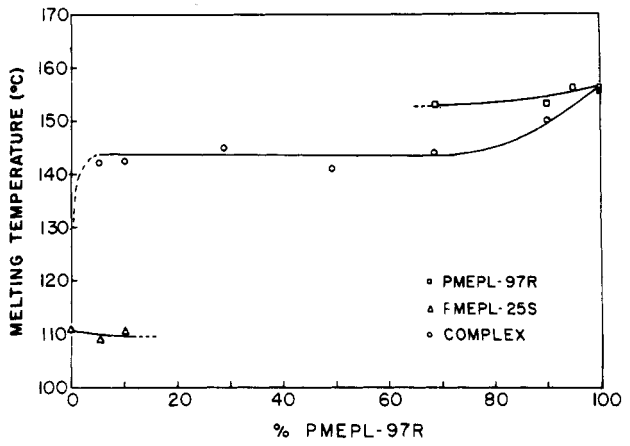

Figure 7. Melting temperature of PMEPL-97R/25S samples crystallized at 80 °C.

the melting peaks of PMEPL-97R and of the stereocomplex are not well resolved, the maxima of the peaks were used, instead of the end of the peaks as in the remainder of this article, to draw Figure 7, which shows a constant value of the melting temperature of the stereocomplex over the major part of the composition range; however, it increases at high concentrations up to the value of PMEPL-97R but decreases at low concentrations down to the value of PMEPL-25S. PMEPL-25S crystallizes when there is less than 15% PMEPL-97R in the mixture, whereas the excess of PMEPL-97R shows a melting peak at PMEPL-97R compositions above 69%. As in the previous case, the crystallization of the stereocomplex is preferred to the crystallization of the two polymers taken separately and hinders the crystallization of the excess polymer.

Figure 8 gives the enthalpy of fusion of PMEPL-97R/25S samples as a function of composition. It should be noted that, in this series, an equimolar blend of *R* and *S* units (given by the vertical dashed line) does not correspond to 50% PMEPL-97R. PMEPL-25S is made of 62.5% *S* units and 37.5% *R* units; equimolarity is obtained

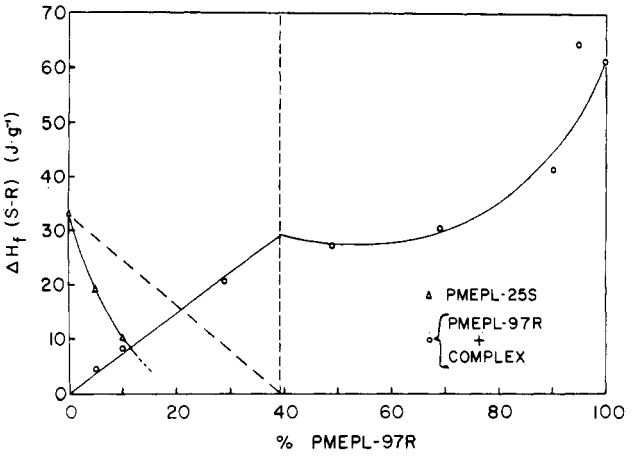

Figure 8. Enthalpy of fusion of PMEPL-97R/25S samples crystallized at 80 °C.

when there is a sufficient amount of isotactic PMEPL-97R added to complex all *S* units of PMEPL-25S; this corresponds to 38.5% PMEPL-97R. For PMEPL-97R/75S mixtures, the equimolar ratio corresponds to 47% PMEPL-97R, which is close to 50%. For PMEPL-97R/99S mixtures, as studied by Grenier and Prud'homme,[7] this corresponds exactly to 50% since the two polymers have the same enantiomeric excess.

Below 38.5% PMEPL-97R, PMEPL-97R/25S blends exhibit a similar behavior (Figure 8) as PMEPL-97R/75S mixtures (Figure 5). The enthalpy of fusion of the stereocomplex increases linearly with compositions up to 29 J/g (extrapolated value) at 38.5% PMEPL-97R (equimolar mixture), whereas the enthalpy of fusion of PMEPL-25S decreases rapidly with composition, up to about 20% PMEPL-97R, above which it cannot crystallize anymore; these latter values are much smaller than those expected (dashed line) considering the amount of PMEPL-25S present in the mixture. At PMEPL-97R concentrations above 38.5% (Figure 8), the enthalpy of fusion increases nonlinearly from 27 to 61 J/g at 100% PMEPL-97R.

Without complexation at all between PMEPL-97R and PMEPL-25S, we would observe a linear variation of the enthalpy of fusion of the 155 °C peak over the full composition range, which would be due to PMEPL-97R uniquely. With stereocomplexation, the enthalpy is expected to increase linearly from 0 to 38.5% since the 155 °C melting peaks corresponds uniquely to the crystallization of the stereocomplex. However, above 38.5%, the melting peak at 155 °C is due to the crystallization of both the stereocomplex and the PMEPL-97R species in excess: the enthalpy of fusion of the first species to crystallize (in this case, we do not know if it is the stereocomplex or PMEPL-97R) must increase linearly with composition, as it does with PMEPL-97R/75S and PMEPL-97R/99S mixtures, but not the second one since its crystallization is hindered by the presence of the crystals originating from the first species. Our results are obviously in agreement with stereocomplexation.

Figure 9 shows the melting curves of PMEPL-97R/0S blends. Three peaks are observed at about 118, 145, and 155 °C corresponding to PMEPL-0S, the stereocomplex (arrows), and PMEPL-97R, respectively. Complexation is not observed below 26% and above 75% PMEPL-97R. PMEPL-0S exhibits a melting peak up to 50% PMEPL-97R, whereas the PMEPL-97R melting peak is present in a composition range going from 15% to 100%. The maxima of the melting peaks of PMEPL-97R/0S blends are plotted in Figure 10 as a function of composition. In this phase diagram, the straight line at 155 °C corresponds

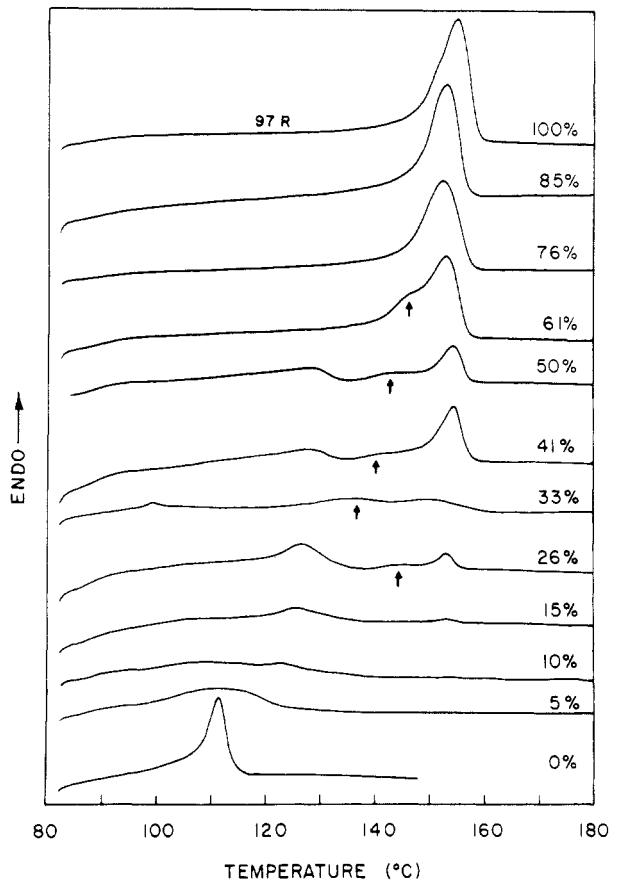

Figure 9. DSC curves of PMEPL-97R/0S samples run at 20 °C/min after crystallization at 80 °C.

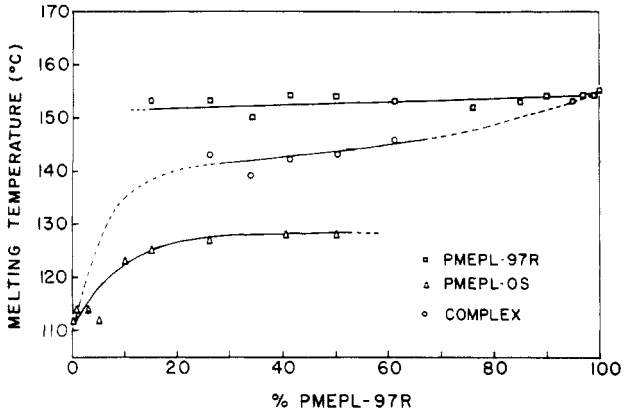

Figure 10. Melting temperature of PMEPL-97R/0S samples crystallized at 80 °C.

to PMEPL-97R, whereas the line at 140 °C is assigned to the stereocomplex which crystallizes in a limited concentration range. Attempts to construct for this system a diagram of the enthalpy of fusion as a function of composition were unsuccessful.

X-ray Diffraction. Grenier and Prud'homme[7] reported different X-ray diffraction patterns for isotactic PMEPL, atactic PMEPL, and the stereocomplex. These patterns can be used as fingerprints to verify the presence or the absence of stereocomplexation with polymers of low isotacticity.

X-ray diffraction patterns of blends containing 50% PMEPL-97R and of the corresponding homopolymers are given in Figure 11. PMEPL-99S and PMEPL-75S samples exhibit a similar pattern which is associated to the isotactic polymer crystal structure. PMEPL-55S, PMEPL-25S, and PMEPL-0S patterns are identical with

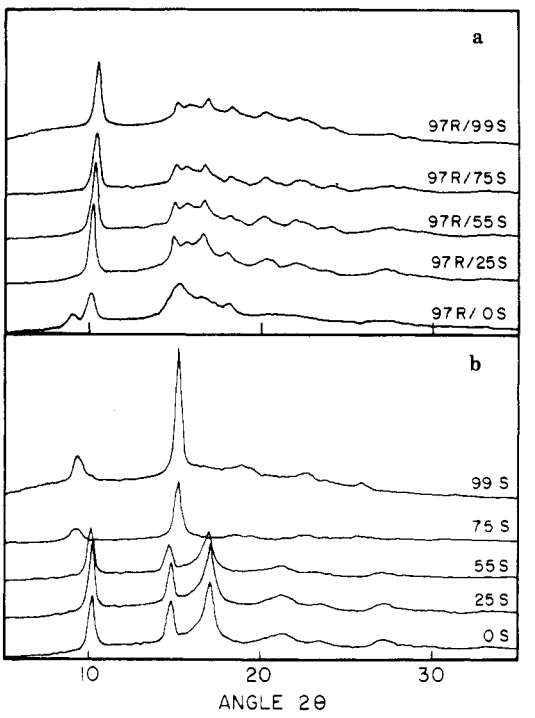

Figure 11. X-ray diffraction traces of PMEPL samples: (a) blends containing 50% PMEPL-97R; (b) pure polymers.

and related to the atactic polymer crystal structure. Grenier and Prud'homme[7] have already shown that these samples exhibit a monoclinic crystal structure in the $P2_1-C_2^2$ space group, with a 2_1 helical chain conformation and slightly different crystal dimensions.

The PMEPL-97R/99S pattern is different from those of the isotactic and atactic polymers (Figure 11) and is characteristic of stereocomplex formation.[7] This same pattern (Figure 11) is also found with PMEPL-97R/75S, PMEPL-97R/55S, and PMEPL-97R/25S samples, confirming complex formation, although part of the atactic diffraction pattern begins to appear in the latter one. The PMEPL-97R/0S sample shows a different behavior; its diffraction pattern is clearly due to more than one species. The two peaks around 10 °C can be assigned to PMEPL-97R/0S and either to PMEPL-97R or to the stereocomplex. Although attempts to determine the origin of these peaks were inconclusive, there are some indications of the presence of a stereocomplex in this blend.

Morphology. Grenier and Prud'homme[7] have already reported a peculiar morphology for PMEPL-97R/99S mixtures, with spherulitic radii of about 500 μm as compared to 4.5 μm for the isotactic polymer and 30 μm for the atactic polymer, all samples being prepared under the same conditions. It was shown that the morphology of the mixtures is controlled by the stereocomplex, which crystallizes first, and leaves the excess polymer trapped in between the lamellae of the spherulites.

The morphology of the mixtures investigated in this work was also studied. The samples were heated at a temperature at least 40 °C above their melting temperature in order to remove previous thermal history. Photomicrographs of slowly cooled blends, each of them containing 50% PMEPL-97R, are given in Figure 12. Characteristic spherulites, due to formation of the stereocomplex, are clearly seen in most cases, and particularly with PMEPL's of high degrees of isotacticity. The spherulitic radii of the complex are about 500 μm for PMEPL-97R/99S, 300 μm for PMEPL-97R/75S, 150 μm for PMEPL-97R/55S, and 75 μm for PMEPL-97R/25S as compared to values below 30 μm for any of the polymers considered to be taken

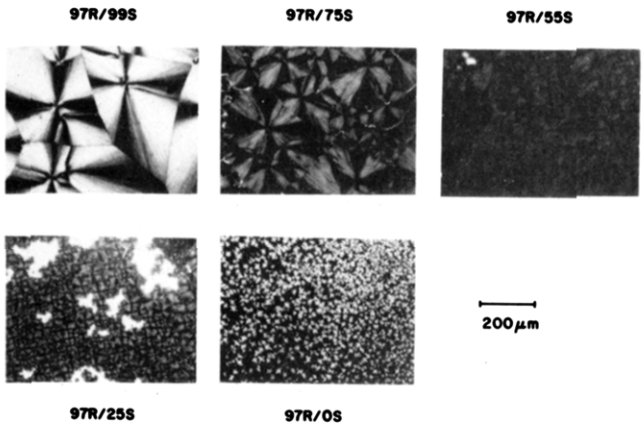

Figure 12. Photomicrographs of blends containing 50% PMEPL-97R, samples crystallized at 0.2 °C/min.

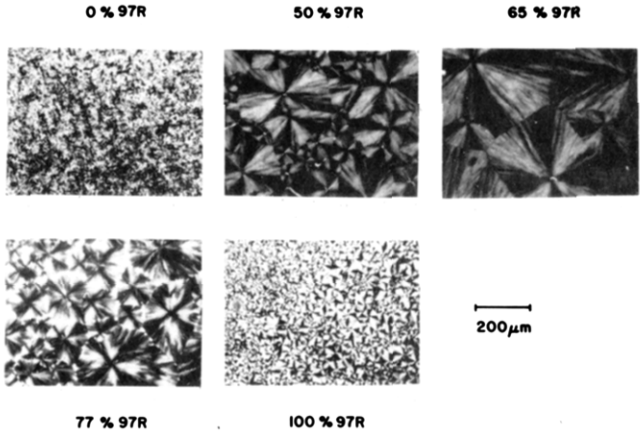

Figure 13. Photomicrographs of PMEPL-97R/75S samples crystallized at 0.2 °C/min.

separately. In the last case (PMEPL-97R/25S), the complex is not volume filling and leaves areas of crystalline isotactic polymer.

Finally, PMEPL-97R/0S does not allow the observation of a different morphology as that observed with the corresponding homopolymers, probably because of the simultaneous crystallization of PMEPL-97R and of the stereocomplex. The complex does not control the morphology in this case, contrary to the previous ones.

Photomicrographs of PMEPL-97R/75S blends, of three different compositions, are given in Figure 13. The morphology of each of these blends is characteristic of the stereocomplex (50% PMEPL-97R) and different from that of the corresponding homopolymers (0 and 100% PMEPL-97R), also shown in Figure 13. The spherulites of the complex containing from 50% to 65% PMEPL-97R are volume filling with a radius of about 300 μm. Above this concentration, the isotactic polymer in excess crystallizes in the free space left between the spherulites of the stereocomplex. This behavior is similar to that of the PMEPL-97R/99S system and characteristic of a strong stereocomplexation.

Photomicrographs of various PMEPL-97R/25S blends are given in Figure 14. PMEPL-25S alone gives a birefringent mass under the polarizing microscope, but no clear morphological entity emerges under the conditions used. PMEPL-97R exhibits highly birefringent but small spherulites. In contrast, the stereocomplex gives, in general, big but low contrasted spherulites. Because of their low contrast, the spherulites of the stereocomplex appear black in Figure 14, but they are closely visible in the polarizing microscope. As a function of the composition of the complex, spherulites begin to appear with only 5% of

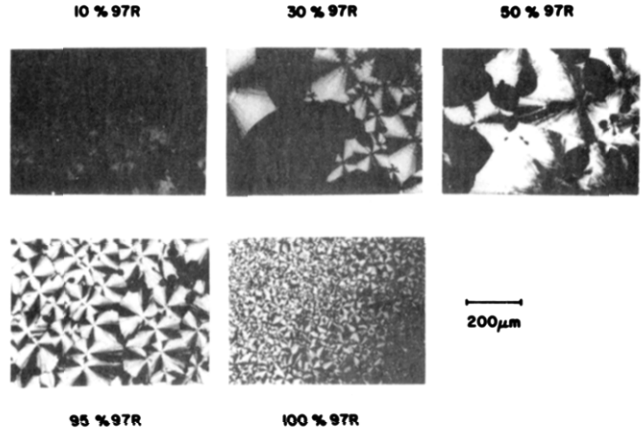

Figure 14. Photomicrographs of PMEPL-97R/25S samples crystallized at 0.2 °C/min.

PMEPL-97R. Above 20% PMEPL-97R, two phases are visible with two types of spherulites which are related to PMEPL-97R and to the stereocomplex. At higher concentrations, the stereocomplex shows up as little black holes within the mass of isotactic polymer spherulites.

These results support the DSC and X-ray measurements given above and confirm the formation of a stereocomplex in PMEPL-97R/99S, PMEPL-97R/75S, and PMEPL-97R/55S mixtures where the spherulites of the complex are volume filling and control the morphology of the sample. With PMEPL-97R/25S, the spherulites of the stereocomplex also crystallize first and control the morphology, but they are not volume filling.

Melting Point Depression Analysis. With copolymers, there is usually a minimum sequence length required to permit the crystallization, and the melting temperature of the copolymer increases with the average sequence length.[11] In this study, stereocomplexes are considered as copolymers made of complexed and uncomplexed units. Their sequence lengths are determined by the initial copolymer composition (for example, sample PMEPL-75S is a statistical copolymer containing 12.5% *R* (configurational) units and 87.5% *S* units; see Table I), and we assume in this analysis the same sequence length for the initial polymer and for the resulting stereocomplex.

Usual crystallization theories assume that statistical copolymers are made of A crystallizable units and B uncrystallizable units. In this study, an isotactic *R* homopolymer is blended with a tactic *S* copolymer, which is made of *S* complexable units and *R* uncomplexable units. The composition of the *S* copolymer is taken as the composition of the complex since there are enough *R* units in the *R* homopolymer to complex all *S* units. As seen before, in Figures 4, 7, and 10, the melting temperature of the stereocomplex depends uniquely upon the *S* copolymer chosen and, with a given copolymer, does not depend upon the composition of the stereocomplex. In other words, it remains the same whether there is an equimolar mixture or an excess of *R* homopolymer added. We can then use copolymer crystallization theories to describe the melting temperature depression data of the stereocomplexes.

There are several theories available to describe the melting point depression data of copolymers. The first one was proposed by Flory,[12] and it reads

$$\frac{1}{T_f} - \frac{1}{T_f^\circ} = \frac{-R}{\Delta H_f^\circ} \ln x \qquad (1)$$

where T_f is the equilibrium melting temperature of the copolymer, T_f° the equilibrium melting temperature of the pure polymer, ΔH_f° the equilibrium enthalpy of fusion, x the molar fraction of crystallizable A units, and R the gas

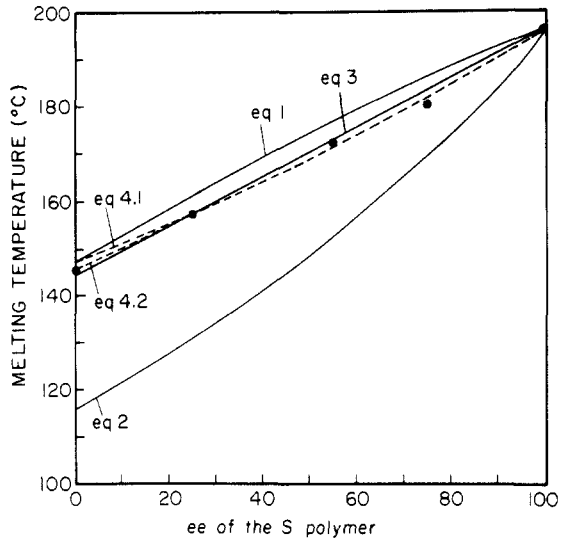

Figure 15. Melting temperature of the stereocomplex as a function of isotacticity.

constant. This equation assumes that a perfectly pure crystal (containing only A units) is in equilibrium with a melt of composition x. The melting point depression is only related to the chemical potential of the melt, which is given by the entropy in this case, and is calculated from the molar fraction. This equation implies the exclusion of uncrystallizable units from the crystal and cannot reasonably explain the complexation with samples of low isotacticity. In this study, we have applied eq 1 and the following ones to the problem of the crystallization of stereocomplexes assuming T_f, the melting temperature of the complex; $T_f°$, the melting temperature of the stereocomplex made between two perfectly isotactic polymers; $\Delta H_f°$, its enthalpy of fusion; and x, the molar fraction of complexable units in the low isotacticity component of the complex.

Baur[13] has proposed a modification of this equation to take into account the average length of crystallizable and uncrystallizable sequences. His equation reads

$$\frac{1}{T_f} - \frac{1}{T_f°} = \frac{-R}{\Delta H_f°}[(\ln x) - (1/L)] \tag{2}$$

where L is the average sequence length. In this case, the chemical potentials have been corrected to consider crystals having a finite thickness (but still containing uniquely crystallizable A units) in equilibrium with equivalent sequence lengths. The melting point depression is larger with this theory than it is with eq 1 which considers crystals of infinite thickness. In fact, the smaller the thickness (or average sequence length), the greater the melting point depression. Although this equation is more realistic and gives better results than eq 1, it does not fit the results of Figure 15 and could not explain the complexation phenomenon of samples of low isotacticity.

To explain those results, we have to use a theory which considers the formation of defects in the crystal. Eby and co-workers[14,15] have proposed an expression which considers an enthalpy of defect formation

$$T_f = T_f°\left(1 - \frac{\Delta \mathrm{Hd}}{\Delta H_f}(1 - x)\right) \tag{3}$$

where ΔHd is the enthalpy of formation of 1 mol of defects. This equation assumes that the crystal and the melt have the same composition. Therefore, in this peculiar case, there is no contribution of the chemical potential of the melt to the melting point depression. When this equation

Table III
Molar Fraction of Uncrystallizable Units in the Crystal (N_c) and Fraction of Uncrystallizable Units Which Have Crystallized (F)

		eq 3[a]	eq 4.1[b]		eq 4.2[c]	
sample	X/%	N_c/%	N_c/%	F/%	N_c/%	F/%
PMEPL-97R/99S	99.5	0.5	0.5	100	0.5	100
PMEPL-97R/75S	87.5	12.5	11	88	12	98
PMEPL-97R/55S	77.5	22.5	18	78	22	95
PMEPL-97R/25S	62.5	37.5	27	63	34	86
PMEPL-97R/0S	50.0	50.0	33	50	43	75

[a] F = 100% and ϵ = ΔHd = 4.9 kJ/mol. [b] ϵ = 6.5 kJ/mol. [c] ϵ = 5.6 kJ/mol.

is fitted to the results of Figure 15, a ΔHd value of 4.9 kJ/mol is obtained, as compared to 22.4 kJ/mol for $\Delta H_f°$.

Sanchez and Eby[16] have proposed a more general equation which takes into account not only the energy involved in the formation of defects but also the composition of the melt, the composition of the crystal, and the difference in chemical potential between those two phases. This equation is

$$\frac{1}{T_f} - \frac{1}{T_f°} = \frac{R}{\Delta H_f°}\left[\frac{N_c\epsilon}{RT_f} + (1 - N_c)\ln\frac{(1 - N_c)}{x} + N_c \ln\left(\frac{N_c}{1 - x}\right)\right] \tag{4}$$

where ϵ is the free enthalpy of incorporation and N_c the molar fraction of uncrystallizable units in the crystal. In this equation, there are two unknown parameters, N_c and ϵ. With a value of zero for N_c, eq 4 reduces to eq 1, which corresponds to a total exclusion of uncrystallizable units. With N_c equal to $1 - x$ (total inclusion), eq 4 reduces to eq 3. In this case, ϵ is equal to ΔHd because there is no segregation between crystallizable and uncrystallizable units and no entropy related to the incorporation.

We, however, believe that these two limiting situations are not realistic and that we need to consider an intermediate level of incorporation. Considering the incorporation of one uncrystallizable unit at one end of each isotactic sequence, we calculate[10]

$$N_c = \frac{[R][S]}{[S] + [R][S]} \tag{4.1}$$

where $[R]$ and $[S]$ are, respectively, the molar fraction of uncrystallizable and crystallizable units in the chain ($[S]$ is equivalent to x). The incorporation of one uncrystallizable unit at each end of each isotactic sequence leads to[10]

$$N_c = \frac{[R][S] + [S][R] - [S][R][S]}{[S] + [R][S] + [S][R] - [S][R][S]} \tag{4.2}$$

Equation 4 is drawn in Figure 15 using eq 4.1 and 4.2, but also in the limit of total inclusion where $N_c = 1 - x$ (eq 3). These three equations give a satisfactory agreement with the experimental values (keeping in mind that there is an adjusting parameter, ϵ). Table III gives, for these three equations, x, the fraction of crystallizable units in the polymer; N_c, the fraction of uncrystallizable units in the crystal; and F, the fraction of uncrystallizable units that have crystallized. With the inclusion of one uncrystallizable unit for each sequence, F is given by[10]

$$F = [S] \tag{5.1}$$

The inclusion of two uncrystallizable units by sequence leads to[10]

$$F = 2[S] - [S]^2 \tag{5.2}$$

With each of these three equations, N_c increases with a decrease of the degree of isotacticity since the larger the amount of uncrystallizable units, the larger the probability of incorporation. The specific values, however, vary slightly (Table III): they go from 0.5% to 50% with eq 3, from 0.5% to 33% with eq 4.1, and are intermediate with eq 4.2, going from 0.5% to 43%. At the same time, the fraction, F, decreases with a decrease in the degree of isotacticity: when there are only a few uncrystallizable units, they can all be included in the crystal; however, an increase of the concentration of impurities causes a rejection from the crystal to preserve its stability.

With these three models, ϵ (or ΔHd) is used as an adjustable parameter to obtain the best fit with the experimental results. With eq 3, where all uncrystallizable units are included in the crystal (F = 100%), ΔHd has been estimated at 4.9 kJ/mol, or 22% $\Delta H_f°$. Equation 4.1 leads to an ϵ value of 6.5 kJ/mol and eq 4.2 to 5.6 kJ/mol.

By use of these three models, the fraction, F, is always high, and the major factor influencing the melting point depression is the $\epsilon/\Delta H_f°$ ratio (in eq 4, the first term in parentheses is much larger than the two other ones). Taking into account the experimental errors, the three models give similar values, the free enthalpy of incorporation being about 5.7 kJ/mol (an average of the three values found with eq 3, 4.1,a nd 4.2), the $\epsilon/H_f°$ ratio being about 0.25 (also an average of three values) and the fraction, F, being at least equal to 50%. However, the best fit is obtained with eq 4.2 (incorporation of two units per sequence), which seems, at the same time, to be a more reasonable model.

Discussion and Conclusions

DSC, morphology, and X-ray diffraction measurements show that PMEPL-97R/99S, PMEPL-97R/75S, PMEPL-97R/55S, and PMEPL-97R/25S mixtures at equimolar ratios give rise to the formation of a stereocomplex between the two tactic polymers involved. The stereocomplexes have higher melting temperatures and exhibit much larger spherulites than their corresponding polymers taken separately; however, these parameters decrease with the degree of isotacticity of the PMEPL-xS (with x = 99, 75, 55, and 25). The stereocomplexes also exhibit a different X-ray diffraction pattern. In all cases, no indication is found of melting peaks, birefringent entities (except for PMEPL-97R/25S), or X-ray diffraction lines due to the initial polymers.

When the concentration of polymer is varied in the mixture, the stereocomplex crystallizes over most of the concentration range, but the excess polymer can only crystallize at high concentrations of the isotactic polymer. The melting temperature of the complex is constant over most of concentration range, whereas its enthalpy of fusion decreases linearly from a maximum for the equimolar mixture to zero. In all cases, at any concentration, the stereocomplex crystallizes first since its crystallization temperature is above that of the excess polymer, hindering the crystallization of the excess polymer, thus reducing its enthalpy of fusion below the value expected, and controlling the morphology of the mixture.

PMEPL-97R/0S blends also form stereocomplexes, but in general, three species seem to crystallize simultaneously: the stereocomplex, PMEPL-97R, and PMEPL-0S. In this case, the stereocomplex does not control the morphology of the mixture.

The melting point depression of the complex as a function of the isotacticity of its components is related to a decrease in the average sequence length of the polymers involved. Indeed, PMEPL-99S, PMEPL-75S, PMEPL-55S, and PMEPL-25S have average sequence lengths of 200, 8, 4.4, and 2.7, respectively. In the latter case, it is surprising to find complexation, owing to the low average sequence length calculated, and melting point depression cannot be directly related to this parameter. We then preferred to use for this purpose the inclusion models proposed by Eby and co-workers[14-16] which increase the effective average sequence length of the polymer used. For example, two short sequences separated by one uncrystallizable unit will show up as a long crystallizable sequence in the inclusion models. The free enthalpy of incorporation, used as an adjustable parameter, has then been estimated at 5.7 kJ/mol, or 0.25 $\Delta H_f°$. It is possible to evaluate the effective sequence length of the polymers used by taking into account the fraction of uncrystallizable units which is included into the crystal. These values have been calculated for the models involving the inclusion of one uncrystallizable unit (eq 4.1) and the inclusion of two uncrystallizable units (eq 4.2) and are given in Table IV; the effective sequence length becomes larger than 10 in most cases. A sequence length of 10 has often been suggested as a limiting value above which crystallization is permitted. However, recent studies of ethylene–vinyl chloride copolymers have indicated that this value can be smaller than 10.[17] Other studies, using a variety of copolymers, indicate a critical sequence length for crystallization between 5 and 15.[18-21]

Table IV
Corrected Molar Fraction and Effective Sequence Length of PMEPL Stereocomplexes

	eq 4.1		eq 4.2	
sample	molar fraction	length	molar fraction	length
PMEPL-99S	100	∞	100	∞
PMEPL-75S	98.5	67	100	400
PMEPL-55S	95	20	99	89
PMEPL-25S	86	7.2	95	19
PMEPL-0S	75	4	88	8

It is unfortunately impossible at this point to describe the interactions occurring between chains of opposite configurations without a knowledge of the crystal structure of the stereocomplex. However, this interaction must be strong enough to allow the incorporation into the crystal of uncrystallizable units with a free enthalpy of incorporation of at least 5 kJ/mol.

Acknowledgment. The authors thank the National Sciences and Engineering Research Council of Canada and the Department of Education of the Province of Québec (FCAR program) for the financial support of this study. The authors are also grateful to Dr. Even Lemieux for fruitful discussions and for reviewing this manuscript.

Registry No. PMEPL-R (homopolymer), 118597-35-6; PMEPL-R (SRU), 80159-48-4; PMEPL-S (homopolymer), 118597-36-7; PMEPL-S (SRU), 80159-49-5; PMEPL-(+–) (homopolymer), 84129-15-7; PMEPL-(+–) (SRU), 84129-16-8; (PMEPL-R)(PMEPL-S), 118597-37-8; (PMEPL-R)(PMEPL-S) (SRU), 118597-38-9.

References and Notes

(1) Jacques, J.; Collet, A.; Wilen, S. H. *Enantiomers, Racemates and Resolutions*; Wiley-Interscience: New York, 1981.
(2) Smith, K. L.; Winslow, A. E.; Peterson, D. E. *Ind. Eng. Chem.* **1959**, *51*, 1361.
(3) Fox, T. G.; Garrett, B. S.; Goode, W. E.; Gratch, S.; Kincaid, J. F.; Spell, A.; Stroupe, J. D. *J. Am. Chem. Soc.* **1958**, *80*, 1768.
(4) Dumas, P.; Spassky, N.; Sigwalt, P. *Makromol. Chem.* **1972**, *156*, 55.
(5) Hatada, K.; Shimizu, S.; Terawaki, Y.; Ohta, K.; Yuki, H. *Polym. J. (Tokyo)* **1981**, *13*, 811.
(6) Ikada, Y.; Jamshidi, K.; Tuji, H.; Hyon, S. H. *Macromolecules* **1987**, *20*, 904.

(7) Grenier, D.; Prud'homme, R. E. *J. Polym. Sci., Polym. Phys. Ed.* **1984**, *22*, 577.
(8) Sakakihara, H.; Takahashi, Y.; Tadokoro, H.; Sigwalt, P.; Spassky, N. *Macromolecules* **1969**, *2*, 515.
(9) Grenier, D.; Prud'homme, R. E.; Leborgne, A.; Spassky, N. *J. Polym. Sci., Polym. Chem. Ed.* **1981**, *19*, 1781.
(10) Lavallée, C. Ph.D. Thesis, Laval University, 1987.
(11) Wunderlich, B. *Macromolecular Physics: Crystal Melting*; Academic Press: New York, 1980; Vol. 3.
(12) Flory, P. J. *Trans. Faraday Soc.* **1955**, *51*, 848.
(13) Baur, H. *Makromol. Chem.* **1966**, *98*, 297.
(14) Colson, J. P.; Eby, R. K. *J. Appl. Phys.* **1966**, *37*, 3511.
(15) Sanchez, I. C.; Eby, R. K. *J. Res. Natl. Bur. Stand. Sect. A* **1973**, *77A*, 353.
(16) Sanchez, I. C.; Eby, R. K. *Macromolecules* **1975**, *8*, 638.
(17) Bowmer, T. N.; Tonelli, A. E. *Polymer* **1985**, *26*, 1195.
(18) Burfield, D. R. *Macromolecules* **1987**, *20*, 3020.
(19) Natta, G.; Mazzanti, G.; Valvassori, A.; Sartori, G.; Morero, D. *Chim. Ind. (Milan)* **1960**, *42*, 125.
(20) Kilian, H. G. *Kolloid Z. Z. Polym.* **1963**, *189*, 23.
(21) Jackson, J. F. *J. Polym. Sci., Part A* **1963**, *1*, 2119.

Polycaprolactone-Based Block Copolymers. 3. Mechanical Behavior of Diblock Copolymers of Styrene and ϵ-Caprolactone

J. Heuschen,† J. M. Vion,‡ R. Jerome,* and Ph. Teyssié

Laboratory of Macromolecular Chemistry and Organic Catalysis, University of Liège, Sart Tilman B6, B-4000 Liege, Belgium. *Received July 7, 1988; Revised Manuscript Received October 19, 1988*

ABSTRACT: Poly(styrene-*block*-ϵ-caprolactone) copolymers (PS–PCL) exhibit a two-phase morphology that dictates their mechanical behavior. The dependence of the isochronous torsion modulus on the copolymer composition clearly shows that a phase inversion takes place at ca. 45 wt % PCL. Although the stress–strain curves are governed by the nature of the continuous phase, the minor component influences the values of stress and strain in each deformation region. At least at compositions close to the phase inversion, the minor component forms semicontinuous phases as supported by electron microscopy and by the mechanical hysteresis of a completely amorphous PS–polyester copolymer comprising 55 wt % polyester. Although brittle at 77 K, a PS–PCL copolymer containing 56 wt % PCL exhibits a ductile fracture when extended by 300%, i.e., when the PCL spherulites are transformed into a microfibrillar structure.

Introduction

Ring-opening polymerization of lactones, lactams, and epoxides bestows on the synthesis of polyesters, polyamides, and polyethers the advantages of chain reactions. Substituting a living polyaddition of cyclic monomers for the usual step-growth process is the best way to control the introduction of the aforementioned chains in block polymers.[1] Living anionic block polymerization of styrene and ethylene oxide is the first likely illustration of that opportunity.[2] A few years ago, a family of bimetallic μ-oxo alkoxides was synthesized as very active anionic coordination-type catalysts in the living polymerization of ϵ-caprolactone (ϵ-CL).[3,4] These catalysts have been successfully modified into polymer (PX) bound catalysts able to produce poly(ϵ-caprolactone) (PCL) containing block polymers (PX-PCL) with well-defined molecular parameters.[5] Among other copolymers, a series of poly(styrene-*block*-ϵ-caprolactone) (PS–PCL) has been synthesized and characterized. Block polymers of composition near 50 wt % of each component display liquid crystalline structures, at room temperature, in the presence of a selective solvent for the amorphous PS block.[6] Phase morphology of bulk copolymers has been investigated by optical and transmission electron microscopy. Monolamellar monocrystals have been prepared by crystallization from highly dilute solutions in a nonsolvent of PCL.[7] How PCL blocks crystallize from the melt has been considered in relation to the molecular weight and composition of the copolymers.[7] The degree of miscibility of PS and PCL, as well as the nature of the continuous phase, has a decisive effect on the crystallization process. A major interest is the potential interfacial activity of PS–PCL copolymers in immiscible PS–PVC blends. Since PCL is known to be miscible with PVC,[8] PS–PCL diblocks might behave as compatibilizers or emulsifiers in these polyblends and improve their poor mechanical properties. The main conclusions of this will be published in the near future. In this paper we address the question of mechanical behavior of PS–PCL diblock copolymers. The discussion will emphasize the effects that phase morphology and especially crystallization of PCL blocks have on the mechanical resistance to deformation and ultimate fracture of these materials.

Table I
Molecular Parameters of the Investigated Poly(styrene-*block*-ϵ-caprolactone) Copolymers

sample	$\bar{M}_n$ PS	$\bar{M}_n$ PCL	PCL, wt %
C1	70 000	35 000	33
C2	70 000	55 000	44
C3	70 000	90 000	56
C4	40 000	100 000	70
Al[a]	90 000	110 000	55

[a] Al comprises a random copolyester block of ϵ-CL and β,δ-dimethyl-ϵ-caprolactone (60%).

Experimental Section

(μ-Oxo)bis[bis(1-methylethoxy)aluminum]zinc was the initial catalyst, the isopropyloxy groups of which were replaced by 2-ethylhexanoate and hydroxy-terminated polystyrene (PS), respectively. The living block polymerization of ϵ-CL proceeded through the selective acyl–oxygen cleavage of the lactone with

* To whom correspondence should be addressed.
† Present address: General Electric Company, Technology Department, Mt Vernon, IN 47620.
‡ Present address: Shell Chemical Research Center, Louvain-la-Neuve, Belgium.

0024-9297/89/2222-2446$01.50/0